

Cloud microphysical and radiative properties for parameterization and satellite monitoring of the indirect effect of aerosol on climate

Jean-Louis Brenguier

Centre National de Recherche Météorologique (CNRM), Météo-France,
Groupe d'étude de l'Atmosphère Météorologique (CNRS-GAME), Toulouse, France

Hanna Pawlowska

Institute of Geophysics, Warsaw University, Warsaw, Poland

Lothar Schüller¹

Institut für Weltraumwissenschaften, Freie Universität Berlin, Berlin, Germany

Received 20 June 2002; revised 5 December 2002; accepted 21 February 2003; published 7 August 2003.

[1] The spatial variability of the microphysical fields in stratocumulus clouds is documented in this paper with statistics of droplet number concentration, droplet mean volume radius, and liquid water content for eight cases of the second Aerosol Characterization Experiment. Statistics are calculated in five sublayers, from cloud base to cloud top, and they are utilized for deriving estimates of cloud optical thickness and liquid water path, by assuming either random or maximum overlap. The resulting in situ frequency distributions of optical thickness and liquid water path are validated against distributions of these two parameters retrieved from independent remote sensing measurements of cloud radiances. They are also used for testing parameterizations of optical thickness based on liquid water path and either the droplet effective radius or the cloud droplet number concentration. This unique data set of extensive, concomitant, and independent measurements of cloud microphysical and radiative properties is finally used for assessing the detectability of the aerosol indirect effect through examination of the correlation between cloud optical thickness and droplet effective radius. If only cases of comparable values of geometrical thickness are considered, the correlation between optical thickness and effective radius is negative, as anticipated by *Twomey* [1977]. However, if the most polluted cases are also accounted for, the trend suggests a positive correlation. In fact, the most polluted cloud systems sampled during ACE-2 were slightly drier, hence thinner, than the marine and intermediate cases, hence producing a positive correlation between optical thickness and droplet effective radius. This study demonstrates that the monitoring of the aerosol indirect effect with satellite observations requires an independent retrieval of the liquid water path together with the cloud optical thickness and droplet effective radius. *INDEX TERMS*: 0320 Atmospheric Composition and Structure: Cloud physics and chemistry; 1610 Global Change: Atmosphere (0315, 0325); 3307 Meteorology and Atmospheric Dynamics: Boundary layer processes; 3359 Meteorology and Atmospheric Dynamics: Radiative processes; 3360 Meteorology and Atmospheric Dynamics: Remote sensing; *KEYWORDS*: stratocumulus, aerosol indirect effect, cloud microphysics, cloud radiative properties, satellite remote sensing, droplet effective radius

Citation: Brenguier, J.-L., H. Pawlowska, and L. Schüller, Cloud microphysical and radiative properties for parameterization and satellite monitoring of the indirect effect of aerosol on climate, *J. Geophys. Res.*, 108(D15), 8632, doi:10.1029/2002JD002682, 2003.

1. Introduction

[2] The aerosol indirect effect (AIE) in boundary layer clouds involves a chain of interactions between aerosol,

cloud dynamics, microphysics, and radiative properties. The injection of anthropogenic aerosols that act as cloud condensation nuclei (CCN) in the natural background involves an increase of the cloud droplet number concentration (CDNC). The resulting increase of cloud optical thickness (COT), at constant liquid water path (LWP), is referred to as the first indirect effect [*Twomey*, 1977]. Modifications of cloud microphysics, however, are likely to also impact cloud dynamics, via the formation of precipitation, and

¹Formerly visiting scientist at Météo-France, Centre National de Recherche Météorologique, Toulouse, France.

therefore the cloud cycle, thus leading to an increase of the cloud lifetime and spatial extent, hence an increase of the mean cloud albedo. This microphysical feedback on cloud dynamics is referred to as the second indirect effect [Albrecht, 1989]. Though the expected albedo enhancement is rather small, its impact at the global scale could be sufficient for counterbalancing part of the warming by greenhouse gases [Houghton *et al.*, 1995]. Improving parameterizations of the AIE and its monitoring from satellite is therefore a key issue in the prediction of climate change.

[3] CLOUDYCOLUMN, one of the five projects in the second Aerosol Characterization Experiment (ACE-2) [Raes *et al.*, 2000], was devoted to the study of the AIE in marine stratocumulus clouds and the strategy was designed as series of column closure experiments [Brenguier *et al.*, 2000b]. The field project took place in June and July 1997, at the vicinity of the Canary Islands. Aerosol physicochemical properties were measured at a surface site, and instrumented aircraft were deployed over the ocean for measurements of the turbulent fluxes in the boundary layer with the UK Met. Research Flight-C130 and the CIRPAS Pelican, microphysical measurements in the stratocumulus cloud layer with the Météo-France Merlin-IV (M-IV), and remote sensing of the cloud radiative properties from above with the DLR-Do-228. The follow-up PACE project (Parameterization of the Aerosol Climatic Effect) was a joint effort between experimentalists and modelers, with the objective of testing existing and developing new parameterizations of the AIE for general circulation models (GCM).

[4] Eight ACE-2 cases are suited for GCM parameterization validation. They are characterized by different aerosol physicochemical properties in the boundary layer, from a marine background to polluted air masses. In these two extreme cases CDNC values range from 50 cm^{-3} to 250 cm^{-3} [Pawłowska and Brenguier, 2000]. In the PACE Topical Issue the physical processes involved in the AIE have first been examined separately, by Guibert *et al.* [2003] and Snider *et al.* [2003] for the interaction between aerosol and cloud microphysics, by Pawłowska and Brenguier [2003] for the impact on precipitation formation, and by Schüller *et al.* [2003] for the impact on cloud radiative properties. The availability of extensive, concomitant, and independent measurements of cloud microphysics from in situ sampling, and cloud radiative properties from remote sensing, is a unique feature of the ACE-2 data set. It is utilized in this paper for testing the consistency of the database that has been built for initialization of CGMs and validation of their parameterizations. In parallel to the modeling approach, satellite monitoring of the AIE is also a requisite step for corroborating the predictions of the models at the global scale. The database is therefore examined for assessing the detectability of the AIE from satellite measurements of cloud radiative properties.

2. Scaling Up Local Measurements to the GCM Resolution Scale

[5] The horizontal resolution of a GCM (from 50 to 200 km) is much larger than the typical scale of individual cloud cells in the boundary layer (from a few hundred

meters to a few km). The GCM vertical resolution ($\sim 100 \text{ m}$) is also larger than the typical evolution scale of cloud microphysics (a few tens of meters for aerosol activation and droplet growth). Therefore boundary layer clouds cannot be resolved explicitly. The purpose of GCM parameterizations is thus to capture the cloud ensemble properties, without accounting for single cell features. An important step in the PACE project was to elucidate relationships between the variables that are used in the models for describing cloud processes and the physical variables that were measured during the ACE-2 field campaign, with a much finer spatial resolution ($\sim 100 \text{ m}$). Guided by this prerequisite, we have developed rigorous statistical procedures for the characterization of each case study, at a scale of 60 km, similar to the spatial resolution of a GCM. This is illustrated by Pawłowska and Brenguier [2003], who define N_{act} as the CDNC value that characterizes the aerosol activation process, and H that represents the cloud geometrical thickness (CGT). Snider *et al.* [2003] evaluate the accuracy of the prediction of N_{act} with a detailed aerosol activation model initialized with the measured aerosol physicochemical properties. Schüller *et al.* [2003] discuss the respective contributions of N_{act} and H to cloud radiative properties (first indirect effect). Pawłowska and Brenguier [2003] examine the feasibility of diagnostic schemes of the cloud system averaged precipitation rate, expressed in terms of N_{act} and H (second indirect effect). In these approaches the stratocumulus is characterized by a single value of each relevant parameter, as if the cloud were uniform.

[6] However, it is also necessary to describe cloud heterogeneity and its impact on cloud processes. Various attempts have been made to address this issue for cloud radiative properties, also referred to as the heterogeneous bias. The effect of horizontal heterogeneity on cloud radiative properties has been tested with statistical models [Barker, 1992; Cahalan *et al.*, 1994a, 1994b, 1995; Davis *et al.*, 1996; Duda *et al.*, 1996; Barker, 1996], showing that heterogeneous clouds have a lower albedo than homogenous ones with the same mean LWP. These approaches start with measurements of relevant parameters and of their natural variability, characterized by their scaling properties. Diverse sets of measurements were used, such as LWP derived from ground radiometers [Cahalan *et al.*, 1995] or the liquid water content (LWC) measured in situ with airborne instruments [Barker, 1992; Davis *et al.*, 1996]. The second step consists of the generation of a virtual cloud field with a cascade model and the last step involves Monte-Carlo simulations of radiative transfer. The efficiency of such statistical models at reproducing vertically organized structures of turbulence in the boundary layer is however limited. An alternative approach is to use large eddy simulation (LES) models [Duda *et al.*, 1996] that explicitly resolve those structures. For the parameterization of precipitation formation at the GCM grid scale, similar approaches are now designed with LES models to examine the cloud ensemble average of the precipitation rate at the GCM scale.

[7] Experimental data sets for validation of the simulated 3-D microphysical fields are rare. In situ measurements only provide a 1-D horizontal characterization of the microphysical fields, with no way to correlate measurements sampled at two different levels in a cloud layer. In contrast, active

remote sensing provides 3-D scanning capabilities, but there is a gap in observing nonprecipitating clouds between lidars that are too rapidly attenuated and millimetric radars that are not sensitive enough to droplets smaller than 10 μm in radius. Some of the in situ drawbacks were overcome with the novel sampling strategy of the instrumented aircraft during ACE-2, which thus provides a unique data set for the characterization of the droplet spatial distribution and its evolution with height above cloud base.

[8] The availability of independent measurements of cloud microphysical (measured in situ with the M-IV) and radiative (remotely measured from the Do-228) properties is another unique feature of the ACE-2 data set. The Twomey inference in fact involves two processes: the influence of modifications of the background aerosol on cloud microphysics on the one hand, and the influence of microphysical changes on cloud radiative properties on the other hand. When Twomey [1977] discussed the possible impact of pollution on global cloud albedo, the first interaction was already confirmed by numerous in situ observations initiated by the early airborne measurements of Warner and Twomey [1967]. The second interaction is harder to assess experimentally because concomitant and independent measurements of microphysics and cloud radiative properties were not available. ACE-2 is the first experiment that provides long samples (more than 3 flight hours, i.e., ~ 800 km) of synchronized and independent measurements of these cloud properties. In situ measurements performed along the flight track, however, cannot be directly compared to remote sensing of cloud radiative properties that reflect the vertical integral of radiative transfer through the cloud layer. To get over this obstacle, in situ data are first stratified vertically with respect to cloud base. Second, statistics of integrated parameters, such as optical thickness and liquid water path, are derived by assuming either random or maximum overlap of the vertically stratified frequency distributions.

3. Vertically Stratified Statistics of Cloud Microphysics

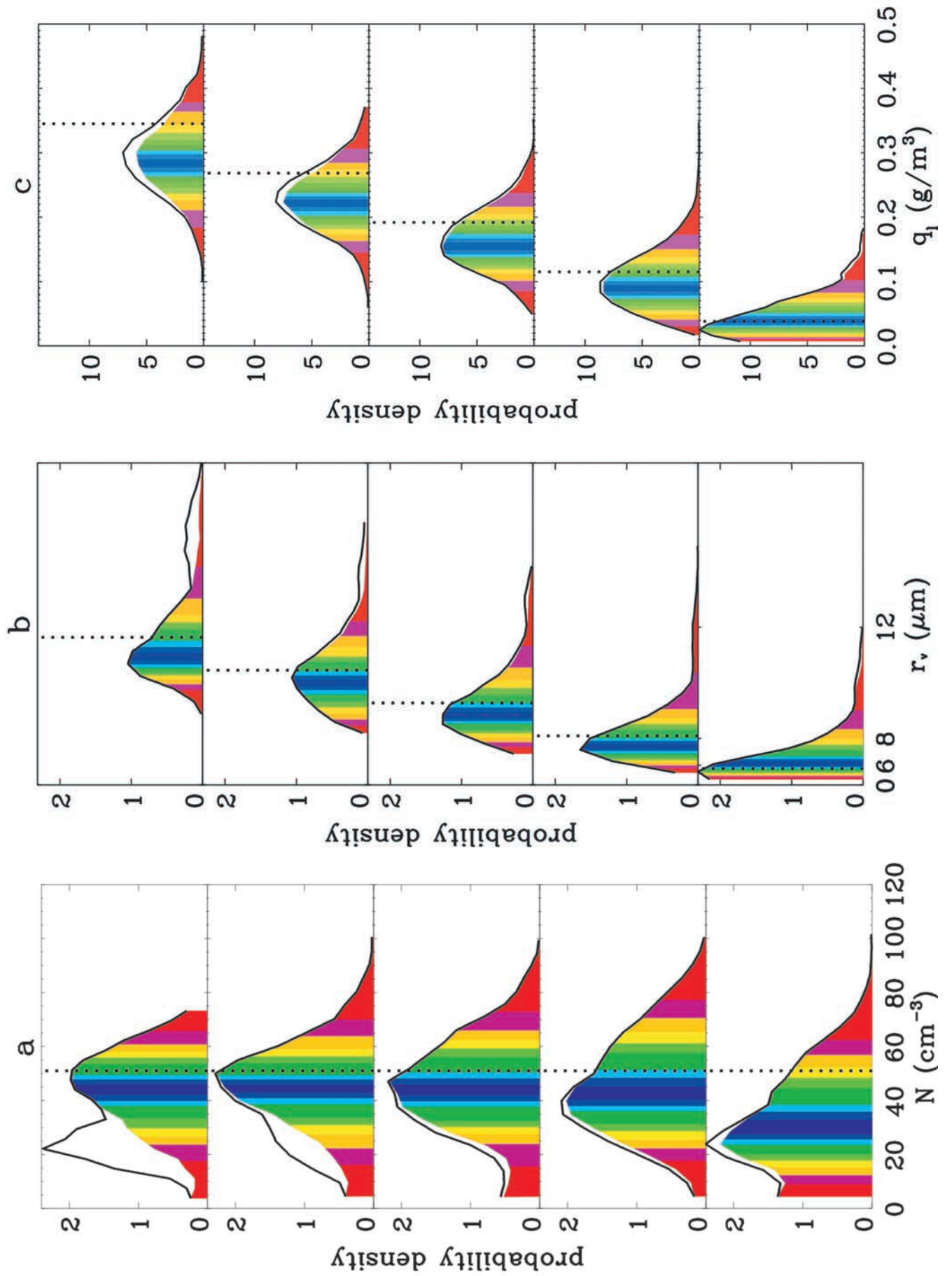
[9] Our analysis is based on the series of ascents and descents performed with the M-IV instrumented aircraft through the stratocumulus layer (see Figure 1 of Pawlowska and Brenguier [2000]). Horizontal legs are rejected in order to avoid oversampling of a particular level within the cloud. Consequently the cumulated flight duration is the same at each level to within a few percent and there is no significant sampling bias. For each study day the cloud layer is divided into five sublayers. The cloud geometrical thickness, as defined by Pawlowska and Brenguier [2003], varies from 272 m on 17 July, to 167 m on 9 July, hence the sublayer thickness varies from $\Delta h = 54.4$ m to 33.4 m. In each sublayer statistics of droplet number concentration N (cm^{-3}), droplet mean volume radius r_v (μm) and liquid water content q_l (g m^{-3}), are calculated from 10 Hz (~ 9 m spatial resolution) cloud samples. The sample selection criteria for statistical significance of the parameters derived from droplet counting and sizing with the Fast-FSSP [Brenguier et al., 1998] are set to $N > 1$ cm^{-3} for the statistics of N (~ 25 droplets actually counted per 0.1 s sample), while statistics of r_v and q_l are restricted to samples with $N > 20$ cm^{-3} (~ 25 droplets actually sized per 0.1 s

sample. Among the droplets counted with the Fast-FSSP, only 5% are accurately sized).

[10] Figure 1 shows the resulting frequency distributions (solid line) for the 26 June case with r_v represented on a cubic scale, that is, proportional to the droplet volume. The color bars indicate the 5% percentiles of the distribution, when drizzle samples (drizzle concentration larger than 2 cm^{-3}) are rejected. The vertical dotted line in the CDNC distribution points to the value N_{act} , defined by Pawlowska and Brenguier [2003] as the value representative of the aerosol activation process for each ACE-2 case. In the r_v and q_l distributions, the lines point to the adiabatic values at each level. It is interesting to note that droplet scavenging by drizzle is more noticeable at the upper levels and that samples with drizzle exhibit N and r_v values respectively smaller and larger than the mean, while they correspond to mean q_l values. Such a feature is only apparent in the clean cases where drizzle production is significant [Pawlowska and Brenguier, 2003].

[11] In Figure 2 the N , r_v and q_l frequency distributions are represented versus height above cloud base, for a clean (26 June) and a polluted (9 July) case. The samples are distributed in five sublayers, as in Figure 1. Statistics are calculated, first over the whole length of ascents and descents through the cloud layer (left column), and second on cloud samples only, defined as samples with $N > 20$ cm^{-3} (right column). The percentage of cloud samples at each level is indicated along the right margins of the two CDNC graphs. We will refer to this percentage as the cloud fraction. In the CDNC distribution the white line indicates the N_{act} value (equal to 51 cm^{-3} and 256 cm^{-3} for 26 June and 9 July, respectively). In the two other graphs it represents the r_v and q_l adiabatic predictions as a function of height above cloud base. The slightly lower CDNC value in the first sublayer is due to an instrumental bias, some of the droplets being smaller than the Fast-FSSP detection threshold (1.3 μm in droplet radius), particularly in the polluted case (9 July). Statistics in the upper sublayers illustrate the effect of entrainment-mixing at cloud top, with a decreasing cloud fraction (left column) and decreasing CDNC values in the cloud samples (right column). However, it can be noted that r_v is less affected by mixing when calculated over cloud samples only. This feature corroborates the assessment that mixing is mostly of the heterogeneous type [Baker et al., 1980]. Note also the good agreement between the adiabatic model predictions and the mean values of the measured r_v and q_l in the right columns where statistics are restricted to the cloud fraction. This figure therefore suggests that the vertical profiles of cloud microphysics can be parameterized with the adiabatic model when only cloud samples are accounted for, the cloud fraction being considered separately. The same analysis was conducted for the eight ACE-2 selected case studies and it is available for validation of GCM and LES models.

[12] The maximum percentage of cloud samples is similar in both cases (90%) and it is observed in the second sublayer above cloud base. The data of a CASI sensor (Compact Airborne Spectrographic Imager), which was installed on board the Do-228, show slightly lower values of 78% on 26 June and 76% on 9 July [Schröder et al., 2002]. This bias suggests that the cloud mask used for CASI data processing and the retrieval of cloud fraction is more



26 JUNE

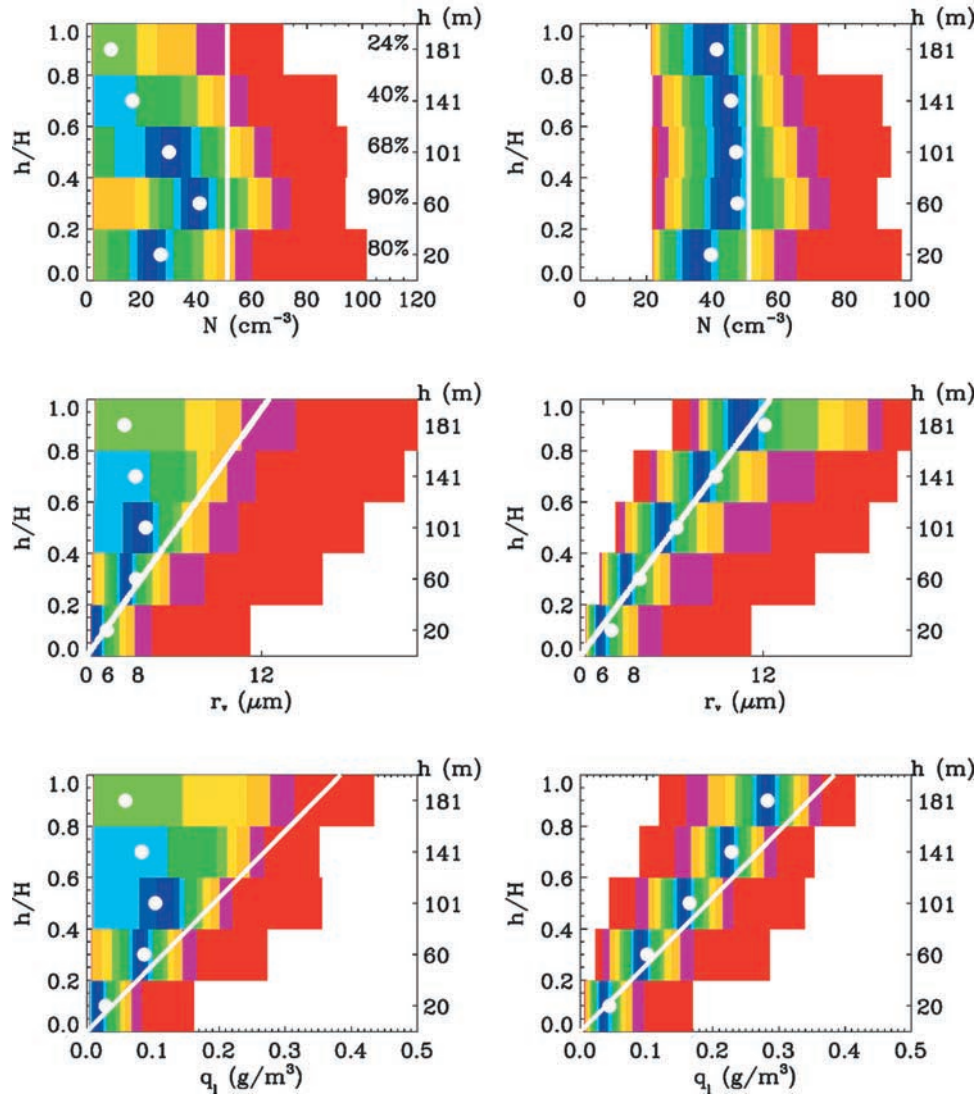


Figure 2. Frequency distributions of N , r_v , and q_l in five sublayers, represented by their 5% percentiles, for the 26 June and 9 July ACE-2 cases. Statistics over the complete duration of the aircraft ascents and descents through the cloud layer are in the left column; statistics limited to cloud samples ($N > 20 \text{ cm}^{-3}$) are in the right column. The mean value in each sublayer is indicated by a white circle. The vertical line in the top row corresponds to the characteristic CDNC value N_{act} (51 cm^{-3} for 26 June and 256 cm^{-3} for 9 July). In the next two rows the lines indicate the adiabatic droplet size prediction, with $N = N_{act}$ in the r_v distribution and the adiabatic LWC in the q_l distribution. The values indicated in the right margins of the CDNC graphs refer to the percentage of cloud samples in each sublayer.

Figure 1. (opposite) Frequency distributions (solid line) of droplet number concentration N , mean droplet volume radius r_v , and liquid water content q_l , for the 10 Hz cloud samples on the 26 June ACE-2 case. Samples from ascents and descents through the cloud layer are distributed into five sublayers, from cloud base to cloud top. The criteria for defining cloud samples are $N > 1 \text{ cm}^{-3}$ for the N distribution, and $N > 20 \text{ cm}^{-3}$ for the r_v and q_l distributions. The color bars indicate the 5% percentiles of the frequency distributions of samples with drizzle concentration smaller than 2 cm^{-3} . The vertical dotted lines point to the characteristic CDNC value N_{act} in the CDNC distribution ($N_{act} = 51 \text{ cm}^{-3}$ for 26 June), to the adiabatic droplet size prediction, with $N = N_{act}$ in the r_v distribution, and to the adiabatic LWC in the q_l distributions.

9 JULY

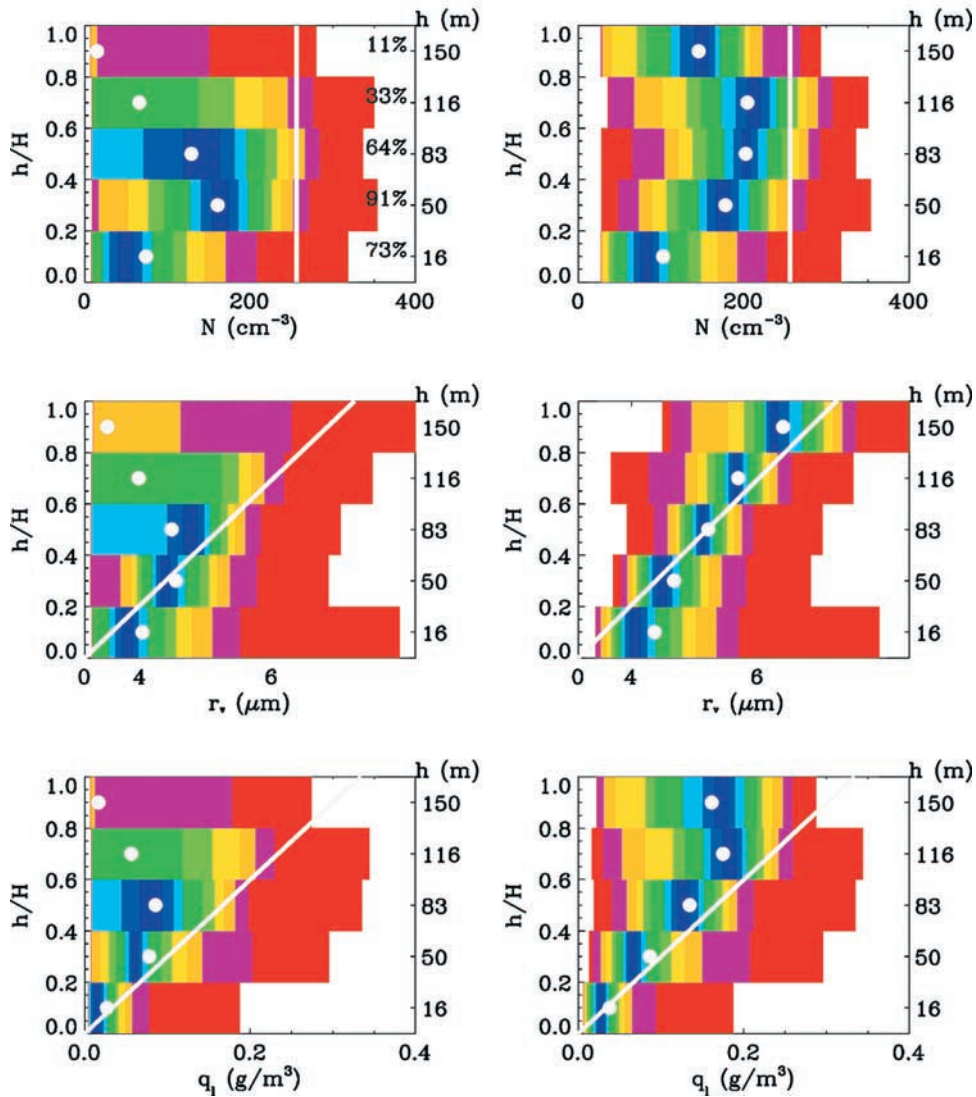


Figure 2. (continued)

restrictive than the cloud selection in the in situ data stratification.

4. Optical Thickness and Liquid Water Path

[13] The optical thickness τ and the liquid water path W (g m^{-2}) are defined as the vertical integrals of the extinction σ_{ext} (m^{-1}) and of q_l , respectively, from cloud base to cloud top:

$$\tau = \int_0^H \sigma_{ext}(h) dh = \int_0^H \pi Q_{ext} N(h) r_s^2(h) dh \quad (1)$$

and

$$W = \int_0^H q_l(h) dh = \int_0^H \frac{4}{3} \pi \rho_w N(h) r_v^3(h) dh, \quad (2)$$

where Q_{ext} is the Mie efficiency factor, ρ_w is the density of bulk water, r_s and r_v are the mean surface and mean

volume droplet radii, respectively, and h is the height above the cloud base. The objective here is to characterize the τ and W frequency distributions from the vertically stratified statistics of the microphysical parameters. With airborne measurements however it is not feasible to correlate measurements made at two separate levels and at different times, so that the above integrals cannot be derived from the series of aircraft ascents and descents through the cloud layer. It is however possible to use statistics of σ_{ext} and of q_l , calculated in five layers and represented by their percentiles, for deriving lower and upper estimates of these frequency distributions. Two models are thus considered for estimating τ and W :

4.1. Random Overlap

[14] The distribution is calculated by assuming that cloud samples overlap randomly in the vertical. $P_{\sigma_{ext}, q_l}(i, n)$ is defined as the i th percentile of the σ_{ext} or q_l frequency distribution, at the n th level. $P_{\tau, W}(j, n)$ is defined as the j th

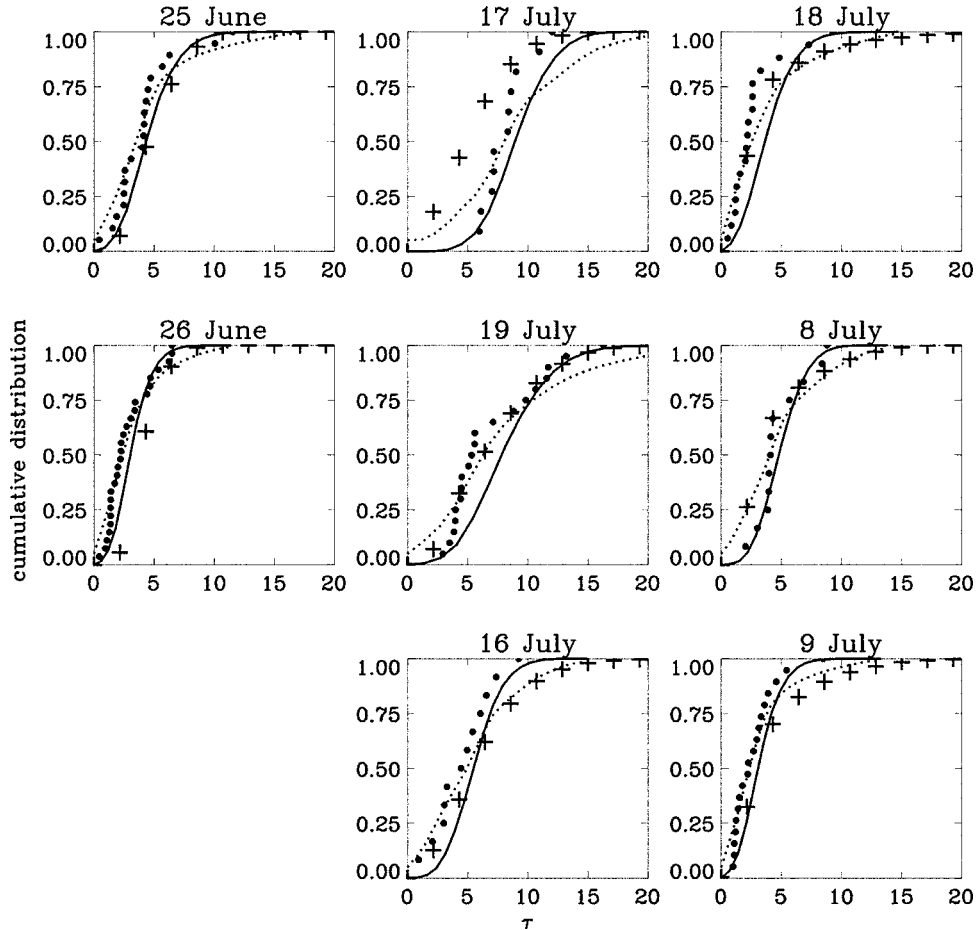


Figure 3. Frequency distributions of cloud optical thickness for the eight cases, based on four estimations: maximum overlap (dotted line), random overlap (solid line), adiabatic prediction (thick dots), and values retrieved from radiance measurements with OVID (plus sign). The left column corresponds to the clean ACE-2 cases, the right column to the most polluted ones, and the middle column to intermediate cases.

percentile of the τ or W distribution after integration of equations (1) or (2), from the cloud base to the n th level. The random overlap model assumes no vertical correlation for $\sigma_{ext}(n)$ or $q_l(n)$. The τ and W distributions are thus calculated iteratively from $n = 1$ to 4, as

$$P_{\tau,W}(j, n+1) = P_{\tau,W}(j, n) + \frac{1}{20} \sum_{i=1}^{20} P_{\sigma_{ext}, q_l}(i, n+1) \Delta h, \quad (3)$$

where $P_{\tau,W}(j, 1) = P_{\sigma_{ext}, q_l}(j, 1) \Delta h$. Such a hypothesis produces the narrowest distributions because randomness smoothes out part of the variability at each level, and it ends with a fairly uniform cloud. Note also that the result depends on the number of sublayers in the vertical stratification. At the limit of an infinite number of sublayers, the random overlap distribution will be reduced to a single value. For model validation, this feature shall therefore be accounted for by considering a model stratification equivalent to that of the database.

4.2. Maximum Overlap

[15] Random overlap of the cloud volumes is not supported by the actual organization of turbulence in the boundary layer. In convective cells updraft generally per-

sist from cloud base to the top. Mixing with overlying dry air at cloud top causes dilution and evaporation of the droplets thus generating downdraft that may penetrate down to the cloud base. Some vertical coherence in the structure of the liquid water content should therefore be expected to be more realistic than a pure random distribution. The highest correlation is expressed by the maximum overlap hypothesis, where the τ or W distribution is calculated as

$$P_{\tau,W}(i) = \sum_{n=1}^5 P_{\sigma_{ext}, q_l}(i, n) \Delta h. \quad (4)$$

This approach produces a much broader distribution, since the lowest τ or W percentile is calculated as the sum of the 5 lowest extinction or LWC percentiles, and similarly for the following percentiles. Figures 3 and 4 show the resulting distributions of COT and LWP, respectively, for the eight ACE-2 cases. In addition to the random and maximum overlap distributions derived from in situ measurements, two additional distributions are displayed. The adiabatic reference is calculated by assuming the cloud layer is made

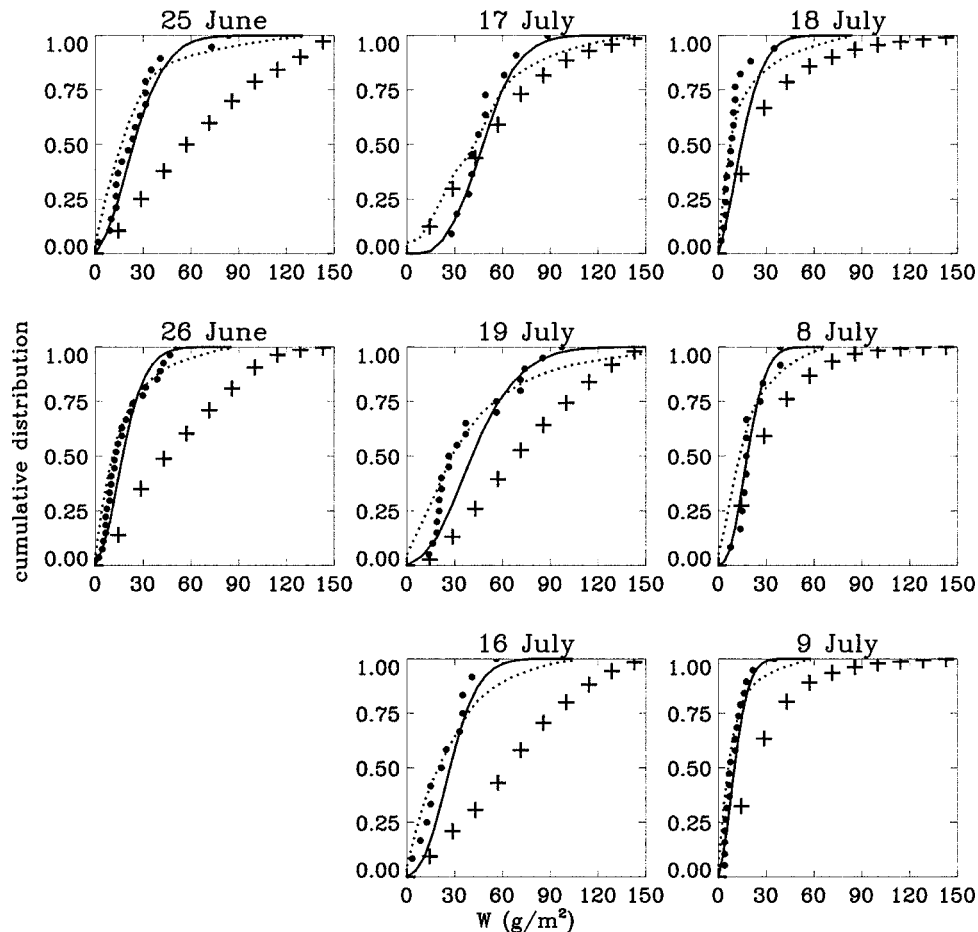


Figure 4. Same as Figure 3 but for liquid water path.

of adiabatic columns with different CGT values. The frequency distribution of H , as derived from each ascent or descent through the cloud layer [Pawlowska and Brenguier, 2003], is thus transformed into an adiabatic τ or W distribution. The second additional distribution was retrieved from radiance measurements with the multi-spectral radiometer OVID [Schüller et al., 2000], as described in Schüller et al. [2003].

[16] Except for the 17 July case the remotely retrieved COT distributions are similar to the distributions built with in situ data, using either the random or maximum overlap hypotheses. In contrast, the retrieved LWP distributions exhibit larger values than the in situ derived distributions for most of the cases. COT and LWP in fact have different status with respect to the retrieval procedure [Schüller et al., 2003]. COT is an optical property of the observed clouds, which is directly derived from the measured radiances. LWP, in contrast, is a microphysical property, that is inferred from the measured radiances by assuming clouds are made of independent adiabatic cloud columns of thickness H . Because W is proportional to H^2 in an adiabatic column, Figure 4 emphasizes the overestimation of the retrieved CGT versus that measured in situ, which is mentioned by Schüller et al. [2003]. Part of the overestimation can be attributed to the fact that discrete in situ sampling of CGT on each profile through the cloud layer is not representative of the continuous sampling with remote

sensing along the leg. Part can be attributed to 3-D radiative effects that are not accounted for by the retrieval technique.

5. Large-Scale Parameterizations

[17] There are two important issues with respect to the variability of cloud microphysics. The first one is the possibility of characterizing an extended cloud system with a minimum set of statistical parameters for each relevant variable, preferably a single one such as the mean value. The second issue is the physical significance of that parameter. A more specific question is to evaluate how a single parameter is capable of reproducing the natural variability of COT and LWP, while preserving the relationships between these two variables that are crucial for the longwave emission and shortwave scattering.

[18] Two parameterizations are tested here. The first one originates from the vertically uniform plane-parallel model:

$$\tau = \frac{3}{2} \frac{W}{\rho_w r_e}, \quad (5)$$

where r_e is the effective radius. The second was derived by assuming LWC increases adiabatically with height above cloud base [Brenguier et al., 2000a]:

$$\tau = \frac{3}{5} \pi Q_{ext} A^{2/3} (kN)^{1/3} H^{5/3} = B(kN)^{1/3} W^{5/6}, \quad (6)$$

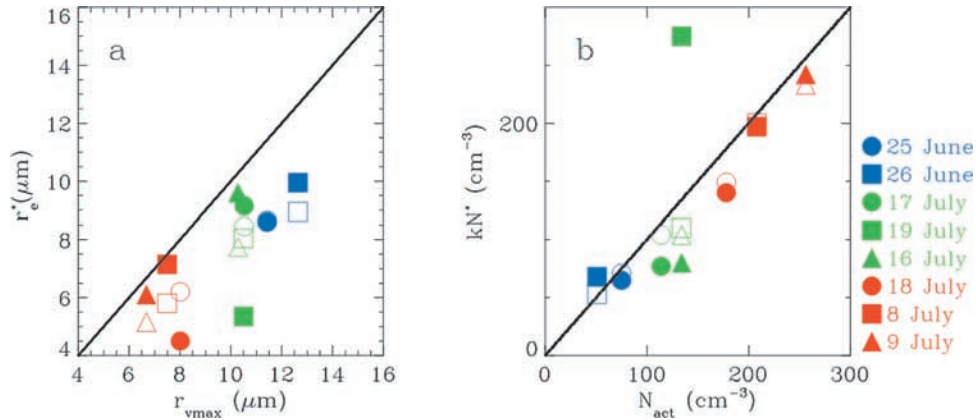


Figure 5. (a) Comparison of the droplet mean volume radius at cloud top r_{vmax} with the droplet radius value r_e^* that minimizes the difference between the measured optical thickness frequency distribution and the one derived from the liquid water path distribution, using equation (5), for both the random (open symbols) and the maximum (filled symbols) overlap distributions. (b) Same for the comparison of the characteristic CDNC value N_{act} with the optimal concentration kN^* , using equation (6).

where A and B are constants that depend on pressure and temperature at cloud base, and k is a parameter that measures the ratio between the mean volume droplet radius and the effective radius ($k = r_v^3/r_e^3$). It varies from 0.8 for clean clouds to $k = 0.9$ for polluted clouds [Pawlowska and Brenguier, 2000].

[19] These two equations establish relationships between two integral variables, τ and W , via a single microphysical parameter that characterizes the impact of pollution on clouds, either the effective radius r_e in equation (5) or the droplet concentration N in equation (6). Parameterization testing was conducted by using the W frequency distribution derived with either the random or the maximum overlap hypothesis, as shown in Figure 4, to calculate a τ distribution, with equation (5), and thus determine the value of r_e that minimizes the difference with the τ distribution derived with the same random or maximum overlap hypothesis, as shown in Figure 3. This optimal value is referred to as r_e^* . The same procedure is repeated with equation (6) for determination of the optimal CDNC value referred to as kN^* . These optimal values are then compared in Figure 5 to the mean volume radius at cloud top r_{vmax} and the CDNC value representative of the aerosol activation process N_{act} , as defined by Pawlowska and Brenguier [2003], for the eight ACE-2 selected cases.

[20] The good agreement between kN^* and the cloud layer characteristic value N_{act} reveals that the COT and LWP distributions derived from in situ measurements are remarkably consistent with the observations of droplet concentration. Of course τ and W being the vertical integrals of the second and third moments of the droplet size distributions, they are not fully independent and some consistency is anticipated, but it is interesting to realize that the physical processes responsible for the variability of the microphysics do not disguise the signature of pollution at the cloud system scale. It can be noted though that the procedure applied to the maximum overlap distributions is not as consistent as the one based on random overlap, while it is expected to be more realistic. The reason is probably due to the fact that the signature of pollution is more detectable in the mean values than in the extremes. The

maximum overlap hypothesis emphasizes the variability and the extreme values, while the random overlap hypothesis tends to smooth the contrast.

[21] The comparison of r_e^* with r_{vmax} also shows more scatter when using the maximum overlap estimates of τ and W . For the random overlap, the best consistency between the τ and W distributions is obtained with an effective radius value close to 80% of the mean volume radius value at cloud top, a ratio comparable to the theoretical value inferred from radiative transfer calculations (83%) by Brenguier *et al.* [2000a].

6. Satellite Monitoring of the AIE

6.1. Methodology

[22] Twomey and Cocks [1989], Nakajima and King [1990], and Nakajima *et al.* [1991] developed procedures for the retrieval of COT and of the droplet effective radius at cloud top (ER) from remote sensing measurements of cloud upward radiances in the visible and near infrared. This technique was the starting point of numerous studies with a strategy based on the identification of a negative correlation between ER and COT, or between ER and cloud albedo, by anticipating that, if such a correlation could be related to changes in the background aerosol, that would corroborate the Twomey [1977] hypothesis and help at quantifying the AIE at the global scale.

[23] Han *et al.* [1994] examined ISCCP data and found “the expected systematic decreases of ER over land compared with over ocean and in the Northern Hemisphere compared with the Southern Hemisphere,” but not the corresponding expected cloud albedo increase. Han *et al.* [1998] extended the statistical approach to the seasonal and geographic variability of cloud albedo and ER, in relation with the LWP variability. They concluded “that cloud albedo increases with decreasing droplet size for most clouds over continental areas and for all optically thicker clouds, but that cloud albedo decreases with decreasing droplet size for optically thinner clouds over most oceans and the tropical forest.” Similar COT and ER retrievals were examined against sulfate burden simulated with a

chemical transport and transformation model [Harsvardhan *et al.*, 2002; Schwartz *et al.*, 2002]. The analysis of two episodes of substantial influx of sulfate aerosol from industrial regions of Europe and North America to remote areas of the North Atlantic revealed “a decrease of ER concomitant with the increase in modeled sulfate burden,” while “cloud optical depth and albedo exhibit little evident systematic trend over the episodes.” Han *et al.* [1998], Harsvardhan *et al.* [2002], and Schwartz *et al.* [2002] speculated that the variability of LWP was the most likely reason for this puzzling observation, but these studies were missing the independent LWP measurements required to corroborate their hypothesis.

[24] Nakajima and Nakajima [1995] concluded from the analysis of AVHRR data collected during FIRE and ASTEX that precipitation formation contributed to a negative correlation between COT and ER. Austin *et al.* [1999], using AVHRR data collected off the coast of California, found a positive correlation, that rather reflects the impact of the LWP variability at constant CDNC. It shall also be noted that multilayer clouds, where ER does not increase with altitude as in a single convective cloud, will further confound COT-ER correlation retrievals based on satellite observations [Schüller, 1999].

[25] Attempts have also been made to test climate numerical simulations against these remote sensing observations. Lohmann *et al.* [2000] corroborate the conclusions of Nakajima and Nakajima [1995] about the role of precipitation formation, while Menon *et al.* [2002] found no relationship between the importance of the simulated AIE and the COT-ER correlation, which is not noticeable in their global simulation. In fact, the crude vertical resolution of the climate models prevents accurate simulation of changes in COT and ER that are related to changes in CGT.

[26] The large variability of the cloud microphysical structure is a serious obstacle to the detection of the Twomey effect. At the small scale (<40 km) aerosol properties are not likely to fluctuate significantly, while cloud dynamical properties do. At this scale COT and RE are positively correlated in response to LWP fluctuations. This feature can be noticed in Figure 8 of Brenguier *et al.* [2000a], especially for the polluted 9 July case. The most reflective cloud cells (COT of 30) exhibit larger ER values (10 μm) than less reflective, hence shallower, cloud cells with ER values decreasing down to <8 μm at COT values lower than 15. Similar results were presented by Boers and Rotstayn [2001] for discussing the various processes that are likely to affect the COT-ER correlation at the small scale. In contrast, significant changes of the aerosol properties can be expected at larger scales in relation with the air mass origin. It is not clear, however, if the effects of the small-scale variability are smoothed out when averaged over a large number of cloud cells, at scales that are relevant for climate studies.

[27] In summary, the experimental confirmation of the Twomey effect requires independent measurements of the cloud microphysical and radiative properties, performed over a range of spatial and timescales sufficiently large for discriminating between the contribution of the in-cloud microstructure variability and the contribution of the background aerosol changes. Such a data set was collected during the SOCEX campaign and analyzed by Boers *et al.* [1998]

for examination of winter versus summer stratocumulus over the Southern Ocean. Their comparison of the remotely measured albedo with that derived from in situ microphysical measurements constitutes an experimental evidence of the Twomey effect. This experiment however was flown with one instrumented aircraft sharing time between in cloud microphysical and above cloud radiative measurements. Boers *et al.* [1998] attribute most of the biases in their comparison to the lack of stationarity of the cloud layer during the course of the in situ and remote sensing flight legs.

[28] The CLOUDCOLUMN experiment was thus designed with a similar strategy as in SOCEX, but using two instrumented aircraft for independent and concomitant measurements of the cloud microphysical and radiative properties. Synchronization of the two aircraft along their trajectory, a 60 km square pattern, was maintained within 100 m (horizontally) and facilitated comparisons of in situ and remote sensing measurements at the scale of single cloud cells. The ACE-2 data are now examined to characterize possible correlations between microphysical and optical cloud parameters at the scale of the cloud system, in order to assess the detectability of the AIE.

6.2. Theoretical Background

[29] As illustrated in Figure 2, the vertical stratification of cloud microphysics is well reproduced by the adiabatic model of convective cell. This feature has been utilized to parameterize cloud radiative properties [Charlson *et al.*, 1987; Bower and Choulaton, 1992; Feingold and Heymsfield, 1992; Boers and Mitchell, 1994; Boers *et al.*, 1998; Brenguier *et al.*, 2000a]. In the adiabatic model, the liquid water content, q_{ad} , can be expressed as a linear function of height h above cloud base [Brenguier, 1991, Appendix B]:

$$q_{ad} = \frac{4}{3} \rho_w N_{ad} r_{vad}^3 = C_w h, \quad (7)$$

where N_{ad} is the CDNC value that is assumed constant in an adiabatic parcel, r_{vad} is the mean volume diameter of the adiabatic droplet size distribution and C_w is the condensation coefficient that depends on pressure and temperature at cloud base. From equations (1) and (7), and assuming a constant ratio between r_{vad} and the adiabatic prediction of the mean droplet surface radius $r_{s,ad}$, τ_{ad} and the effective radius at cloud top, $r_e = r_v^3(H)/r_s^2(H)$ are expressed as power laws of N and H (or W):

$$\tau \propto N^{1/3} H^{5/3} \propto N^{1/3} W^{5/6} \quad \text{and} \quad r_e \propto N^{-1/3} H^{1/3} \propto N^{-1/3} W^{1/6}, \quad (8)$$

where the subscript “ad” has been omitted for simplicity. These relationships have been corroborated at the scale of the cloud cells, with the collocated and independent measurements of cloud microphysics in situ and cloud radiative properties from remote sensing, performed during ACE-2 [Brenguier *et al.*, 2000a].

[30] At constant LWP, this set reduces to $d\tau/\tau = -dr_e/r_e$, which is the basis of the discussion by Han *et al.* [1998]. However, equation (8) shows that the correlation between COT and ER is altered when H or W fluctuate, as they do in actual cloud fields. In order to interpret the ACE-2 results, a

Table 1. Summary of the Eight ACE-2 Selected Cases Characterization^a

Date	Symbol	N , cm^{-3}	H , m	r_e , μm	τ
26 June	solid square	51	202	12.6	4.88
25 June	solid circle	75	262	11.4	5.46
17 July	shaded circle	114	272	10.5	5.44
19 July	shaded square	134	272	10.5	6.86
16 July	shaded triangle	134	222	10.3	6.10
18 July	open circle	178	192	8.01	3.84
8 July	open square	208	182	7.50	4.53
9 July	open triangle	256	167	6.68	4.16

^aSymbols as in Figure 6.

possible correlation between H and N is represented by the coefficient γ :

$$H \propto N^\gamma. \quad (9)$$

In such a case, τ and r_e variations are related to CDNC variations as

$$\frac{d\tau}{\tau} = \frac{1}{3}(5\gamma + 1)\frac{dN}{N} \quad \text{and} \quad \frac{dr_e}{r_e} = \frac{1}{3}(\gamma - 1)\frac{dN}{N}. \quad (10)$$

The correlation between τ and r_e thus expresses as

$$(\gamma - 1)d\tau/\tau = (5\gamma + 1)dr_e/r_e, \quad (11)$$

which establishes two regimes for the correlation:

$$\begin{aligned} -1/5 < \gamma < 1 &\Rightarrow \frac{d\tau/\tau}{dr_e/r_e} < 0 \quad \text{and} \\ \gamma < -1/5 \quad \text{or} \quad \gamma > 1 &\Rightarrow \frac{d\tau/\tau}{dr_e/r_e} > 0. \end{aligned} \quad (12)$$

This result indicates that a negative correlation between τ and r_e can only be expected if H and N are not, or only slightly, correlated [$-1/5 < \gamma < 1$]. The case $\gamma = 0$ (constant H) corresponds to the simplified description of the AIE mentioned above, with $d\tau/\tau = -dr_e/r_e$. Various phenomena can be put forward to assert such a correlation between cloud morphology and cloud microphysics. For example, in a cumulus field updraft speed is generally stronger in the deepest cells. Since strong updraft contribute to the activation of smaller and numerous CCN, such a process implies a positive correlation between H and N . At a larger scale, one should recognize that different aerosol backgrounds originate from different air mass trajectories, oceanic origin for the lowest droplet concentrations as opposed to continental origin for the largest ones. The surface water vapor fluxes being generally reduced over the continent, it is likely that continental air masses are correlated with drier and thinner cloud layers, hence a negative correlation between H and N is expected. The analysis of the ACE-2 data set supports this second scenario.

6.3. Results

[31] Table 1 summarizes the cloud system characterization of the eight ACE-2 selected cases. Cloud microphysical properties are taken from *Pawlowska and Brenguier* [2003]. N_{act} is used for characterizing the CDNC cloud system value N . H is the cloud geometrical thickness. The maxi-

mum mean volume droplet radius r_{vmax} is used as a surrogate for the effective radius at cloud top r_e . The independent measurement of COT comes from *Schüller et al.* [2003]. The cloud system optical thickness is represented by the logarithmic mean of the COT frequency distribution to account for the nonlinear relationship between COT and cloud albedo.

[32] The 25 and 26 June and 16, 17, and 19 July cases show a geometrical thickness >200 m. If these five cases only are considered (black and gray symbols), the COT-ER correlation (Figure 6d) is negative, as predicted by *Twomey* [1977]. However, if the three additional polluted cases are accounted for (open symbols), there is a noticeable decreasing trend of H with increasing N , following a $H \propto N^{-1/2}$ power law, as illustrated in Figure 6a. It is not intended here to pretend that such a correlation is a universal feature. It is likely that the relationship between N and H would have been quite different in another geographical location and that the value $\gamma = -1/2$ is fortuitous, as attested by the 26 June case. However, this negative H - N correlation reflects a real phenomenon that was experienced during the whole ACE-2 campaign. *Verver et al.* [2000] have shown that pollution outbreaks at Tenerife can be traced back to either the UK, France, or the Iberian Peninsula. Because of their continental origin these air masses were drier than air masses originating from the North Atlantic. The cloud layers sampled during pollution outbreaks over the area were thus thinner than the pure marine cases.

[33] If the three polluted cases are not accounted for, Figures 6b and 6c for r_e and τ , respectively, show the expected trends for $\gamma = 0$: $r_e \propto N^{-1/3}$ and $\tau \propto N^{-1/3}$. With these three cases included they rather suggest $r_e \propto N^{-1/2}$ and $\tau \propto N^{-1/2}$, as expected with a γ value of $-1/2$. Because of the systematic decrease of H with increasing N , the r_e decrease is stronger than expected, while τ shows a decrease instead of the expected increase. As a result, the correlation between τ and r_e is positive, as shown in Figure 6d, instead of being negative as anticipated with the constant W formulation.

6.4. Discussion

[34] Various hypotheses were discussed in the literature to account for positive or negative correlations between the remotely retrieved values of COT and ER. As previously mentioned by *Han et al.* [1998] the remote observation of clouds with different CGT, but the same CDNC values (equivalent in equation (6) to $1/\gamma = 0$) will obviously produce a positive correlation between COT and ER ($\tau \propto r_e^5$). This is corroborated at the small scale by the ACE-2 data set when each case is considered separately. Figure 8 of *Brenguier et al.* [2000a] illustrate this feature for the cleanest and the most polluted cases: COT and ER are positively correlated within each cloud system due to the variability of CGT, while CDNC and more generally the aerosol properties do not vary significantly.

[35] It is also particularly relevant to explore possible correlations between COT, ER, CDNC and CGT values characterizing each cloud system as a whole. ACE-2 provides eight cases from very clean to significantly polluted aerosol background. Characteristic values have been calculated with rigorous statistical procedures. The analysis reveals some occurrence of a negative correlation between

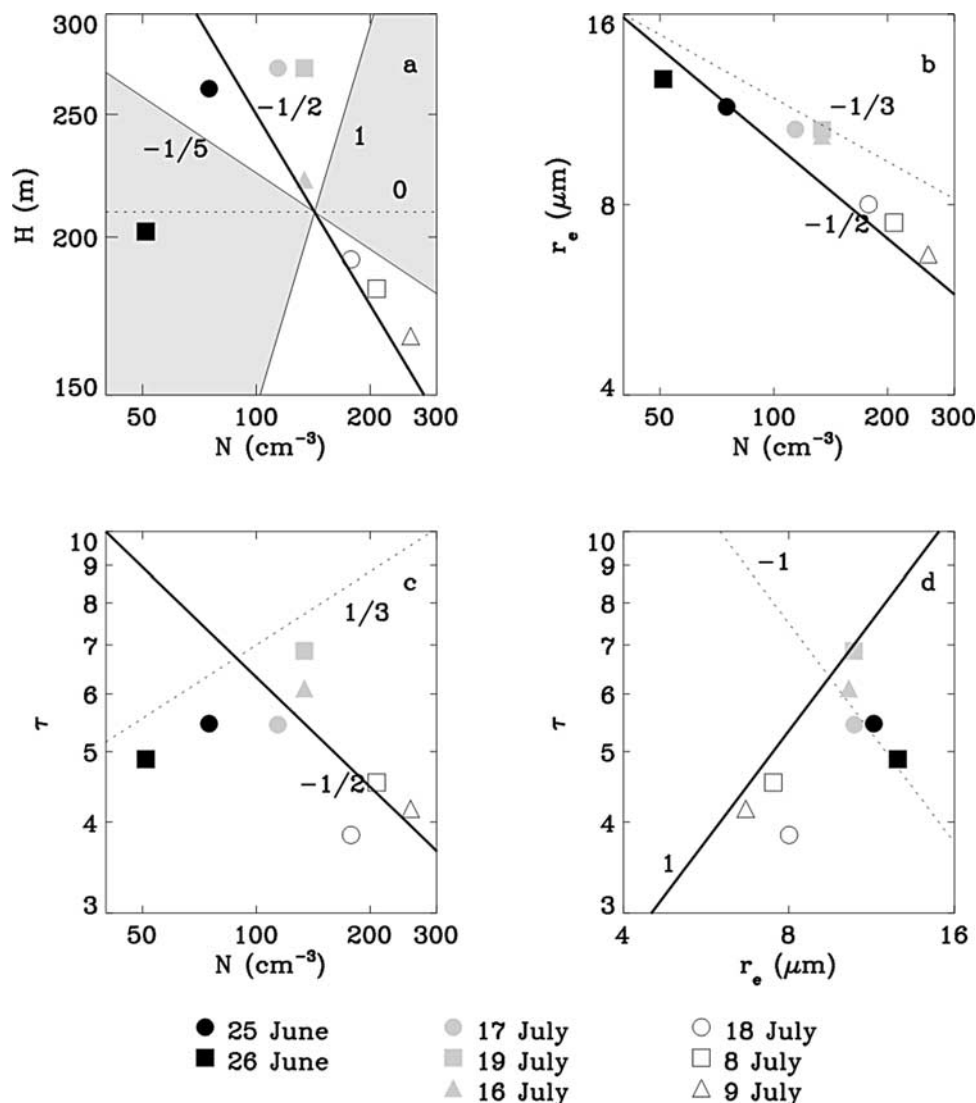


Figure 6. Correlations between the H , N , r_e , and τ characteristic values of the eight ACE-2 cases. (a) Thin lines indicate the γ limits ($\gamma = -1/5$) and ($\gamma = 1$) for a negative correlation between r_e and τ (gray area), and the solid line is the best fit ($\gamma = -1/2$), with the 26 June case excluded. (b–d) Dotted line is the expected correlation exponent, if H or W is constant ($\gamma = 0$). The solid line characterizes the expected correlation exponent with $\gamma = -1/2$.

CDNC and CGT. In fact such a correlation is likely to occur at the scale of a cloud system, because changes in the aerosol background at a given location are associated to changes in the air mass trajectories, hence the thermodynamics. The data set also demonstrates that the H - N correlation is sufficient for counterbalancing the Twomey effect and for producing a positive COT-ER correlation. It is not obvious that these results can be generalized to the global scale, but they demonstrate that combined observations of τ and r_e are not sufficient for assessing or quantifying the AIE and the origin of the observed correlations between COT and ER. Equation (12) indicates that the condition for the expected negative COT-ER correlation is in fact very narrow [$-1/5 < \gamma < 1$]. If H and N are correlated, either positively (with $\gamma > 1$) or negatively (with $\gamma < -1/5$), COT and ER are likely to be positively correlated according to equation (12).

[36] A positive correlation does not imply that the AIE does not exist. It only suggests that continental air masses transported over the ocean can be characterized by lower optical thickness than pure marine air masses at the same location, despite their enhanced droplet number concentration. The AIE refers to a different process, namely that anthropogenically polluted clouds have a higher albedo than similar clouds in the preindustrial era.

7. Conclusion

[37] The processing of the ACE-2 data has been extended in this paper to the characterization of the variability of the microphysical fields in the sampled cloud layers, with emphasis on the vertical stratification. Examples for the cleanest and the most polluted ACE-2 cases are provided, with statistics of CDNC, mean droplet volume radius and

LWC, stratified into five altitude levels. They illustrate the effects of mixing with dry air and drizzle scavenging on droplet spectra. They also confirm that the adiabatic predictions of the droplet mean volume radius and LWC provide a realistic representation of the vertical cloud structure.

[38] The layer-stratified statistics are used for deriving estimates of cloud optical thickness and liquid water path, by assuming either random or maximum overlap of the extinction and liquid water content distributions in the vertical. The comparison with the statistics of the values retrieved from remote sensing shows a good agreement for COT, while remotely retrieved values of LWP are over-estimated with respect to the values derived from in situ sampling. COT is an optical property of the clouds that is directly retrieved from remote sensing of cloud radiances. The similarity of the remotely retrieved and in situ derived statistics of COT attests to the consistency of the ACE-2 data set. In contrast LWP is inferred by assuming that the cloud layer is a mosaic of independent adiabatic cloud columns. The discrepancy between the remotely retrieved and the in situ derived statistics reveals either that the two sampling procedures (continuous sampling along the flight leg for remote sensing versus a few discrete estimations of CGT and LWP on each cloud traverse for in situ sampling) may not be compatible, or that the LWP retrieval technique is biased, possibly due to 3-D radiative effects that are not accounted for by the independent pixel adiabatic model. Because LWP is a crucial parameter that governs both cloud radiative transfer and precipitation formation, significant investments should be devoted to independent measurements of this parameter in future field experiments.

[39] The in situ derived statistics of COT and LWP are also examined for internal consistency with regard to current GCM parameterizations, using either effective droplet radius or droplet concentration, to determine if a single “layer equivalent” value of these parameters is able to reconcile the observed COT and LWP variability. It is found that the “equivalent” effective radius is of the order of 80% of the mean droplet volume radius at cloud top, as inferred from previous radiative transfer calculations by *Brenguier et al.* [2000a]. For CDNC the “equivalent” value kN^* is similar to the value of droplet concentration N_{act} that characterizes the aerosol activation process in each cloud system [*Pawlowska and Brenguier*, 2003].

[40] Finally the respective contributions of CGT and CDNC to the correlation between COT and ER have been clarified at the scale of the cloud systems, with the measurements of cloud morphology, microphysics, and radiative properties that were performed independently and simultaneously during ACE-2. It is shown that the negative correlation between COT and ER (Twomey effect) is noticeable when comparing cloud layers of similar geometrical thickness. During ACE-2 however, the most polluted cases were characterized by thinner cloud layers than the marine ones, because of their continental origin. Such a correlation between CDNC and CGT is sufficient for counterbalancing the impact of CDNC on COT, hence resulting in a positive correlation between COT and ER. Satellite monitoring of these effects will thus become feasible at the global scale when independent measurements

of cloud radiative properties and liquid water path are made available.

[41] **Acknowledgments.** The authors acknowledge the help of the members of the PACE group. Their contributions to the data analysis and interpretation, and to the editorial work is most appreciated. This work is supported by the European Union under grant EVK2-CT-1999-00054, by Météo-France, by the Polish State Committee for Scientific Research (KBN) under grant SPUB-M, and by the Freie Universität Berlin.

References

- Albrecht, B. A., Aerosols, cloud microphysics, and fractional cloudiness, *Science*, 245, 1227–1230, 1989.
- Austin, P. H., M. Szczodrak, and G. M. Lewis, Spatial variability of satellite-retrieved optical depth and effective radius in marine stratocumulus clouds, paper presented at the 10th Conference on Atmospheric Radiation, Madison, Wisconsin, 28 June–2 July, 1999, Am. Meteorol. Soc., Madison, Wis., 1999.
- Baker, M. B., R. G. Corbin, and J. Latham, The influence of entrainment on the evolution of cloud-droplet spectra: I. A model of inhomogeneous mixing, *Q. J. R. Meteorol. Soc.*, 106, 581–598, 1980.
- Barker, H. W., Solar radiative transfer through clouds possessing isotropic variable extinction coefficient, *Q. J. R. Meteorol. Soc.*, 118, 1145–1162, 1992.
- Barker, H. W., Estimating cloud field albedo using one-dimensional series of optical depth, *J. Atmos. Sci.*, 53, 2826–2837, 1996.
- Boers, R., and R. M. Mitchell, Absorption feedback in stratocumulus clouds: Influence on cloud top albedo, *Tellus, Ser. A*, 46, 229–241, 1994.
- Boers, R., and L. D. Rotstajn, Possible links between cloud optical depth and effective radius in remote sensing observations, *Q. J. R. Meteorol. Soc.*, 127, 2367–2382, 2001.
- Boers, R., J. B. Jensen, and P. B. Krummel, Microphysical and short-wave radiative structure of stratocumulus clouds over the Southern Ocean: Summer results and seasonal differences, *Q. J. R. Meteorol. Soc.*, 124, 151–168, 1998.
- Bower, K. N., and T. W. Choullarton, A parameterization of the effective radius of ice free clouds for use in global climate models, *Atmos. Res.*, 27, 305–339, 1992.
- Brenguier, J. L., Parameterization of the condensation process: A theoretical approach, *J. Atmos. Sci.*, 48, 264–282, 1991.
- Brenguier, J. L., T. Bourriane, A. Coelho, J. Isbert, R. Peytavi, D. Trevarin, and P. Wechsler, Improvements of droplet size distribution measurements with the Fast-FSSP, *J. Atmos. Oceanic Technol.*, 15, 1077–1090, 1998.
- Brenguier, J. L., H. Pawlowska, L. Schüller, R. Preusker, J. Fischer, and Y. Fouquart, Radiative properties of boundary layer clouds: Droplet effective radius versus number concentration, *J. Atmos. Sci.*, 57, 803–821, 2000a.
- Brenguier, J. L., P. Y. Chuang, Y. Fouquart, D. W. Johnson, F. Parol, H. Pawlowska, J. Pelon, L. Schüller, F. Schröder, and J. R. Snider, An overview of the ACE-2 CLOUDYCOLUMN Closure Experiment, *Tellus, Ser. B*, 52, 814–826, 2000b.
- Cahalan, R. F., W. Ridgway, J. W. Wiscombe, and T. L. Bell, The albedo of fractal stratocumulus clouds, *J. Atmos. Sci.*, 51, 2434–2455, 1994a.
- Cahalan, R. F., W. Ridgway, and J. W. Wiscombe, Independent pixel and Monte Carlo estimates of stratocumulus albedo, *J. Atmos. Sci.*, 51, 3776–3790, 1994b.
- Cahalan, R. F., D. Silberstein, and J. B. Snider, Liquid water path and plane-parallel albedo bias during ASTEX, *J. Atmos. Sci.*, 52, 3002–3012, 1995.
- Charlson, R. J., J. E. Lovelock, M. O. Andreae, and S. G. Warren, Oceanic phytoplankton, atmospheric sulphur, cloud albedo and climate, *Nature*, 326, 655–661, 1987.
- Davis, A., A. Marshak, J. W. Wiscombe, and R. Cahalan, Scale invariance of liquid water distributions in marine stratocumulus. Part I: Spectral properties and stationarity issues, *J. Atmos. Sci.*, 53, 1538–1558, 1996.
- Duda, D. P., G. L. Stephens, B. Stevens, and W. R. Cotton, Effects of aerosols and horizontal inhomogeneity on the broadband albedo of marine stratus: Numerical simulations, *J. Atmos. Sci.*, 53, 3757–3769, 1996.
- Feingold, G., and A. J. Heymsfield, Parameterizations of condensational growth of droplets for use in general circulation models, *J. Atmos. Sci.*, 49, 2325–2342, 1992.
- Guibert, S., J. J. Snider, and J.-L. Brenguier, Aerosol activation in marine stratocumulus clouds: 1. Measurement validation for a closure study, *J. Geophys. Res.*, 108(D15), 8628, doi:10.1029/2002JD002678, in press, 2003.
- Han, Q., W. B. Rossow, and A. A. Lacis, Near-global survey of effective droplet radii in liquid water clouds using ISCCP data, *J. Clim.*, 7, 465–497, 1994.

- Han, Q., W. B. Rossow, J. Chou, and R. M. Welch, Global survey of the relationship of cloud albedo and liquid water path with droplet size using ISCCP, *J. Clim.*, *11*, 1516–1528, 1998.
- Harsvardhan, S. E. Schwartz, C. M. Benkovitz, and G. Guo, Aerosol influence on cloud microphysics examined by satellite measurements and chemical transport modelling, *J. Atmos. Sci.*, *59*, 714–725, 2002.
- Houghton, J. T., L. G. Meira Filho, B. A. Callander, and N. Harris, A. Kattenberg, and K. Maskell (Eds.), *IPCC 95: Climate Change 1995, The Science of Climate Change, Contribution of the Scientific Assessment Working Group (WGI) to the Second Assessment Report of the Intergovernmental Panel on Climate Change*, 572 pp., Cambridge Univ. Press, New York, 1995.
- Lohmann, U., G. Tselioudis, and C. Tyler, Why is the cloud albedo-particle size relationship different in optically thick and optically thin clouds?, *Geophys. Res. Lett.*, *27*, 1099–1102, 2000.
- Menon, S., A. D. Del Genio, D. Koch, and G. Tselioudis, GCM simulations of the aerosol indirect effect: Sensitivity to cloud parameterization and aerosol burden, *J. Atmos. Sci.*, *59*, 692–713, 2002.
- Nakajima, T., and M. D. King, Determination of the optical thickness and effective particle radius of clouds from reflected solar radiation measurements, Part I: Theory, *J. Atmos. Sci.*, *47*, 1878–1893, 1990.
- Nakajima, T., and T. Nakajima, Wide-area determination of cloud microphysical properties from NOAA AVHRR measurements for FIRE and ASTEX regions, *J. Atmos. Sci.*, *52*, 4043–4059, 1995.
- Nakajima, T., M. D. King, J. D. Spinhrne, and L. F. Radke, Determination of the optical thickness and effective particle radius of clouds from reflected solar radiation measurements. Part II: Marine stratocumulus observations, *J. Atmos. Sci.*, *48*, 728–750, 1991.
- Pawlowska, H., and J. L. Brenguier, Microphysical properties of stratocumulus clouds during ACE-2, *Tellus, Ser. B*, *52*, 867–886, 2000.
- Pawlowska, H., and J.-L. Brenguier, An observational study of drizzle formation in stratocumulus clouds for general circulation model (GCM) parameterizations, *J. Geophys. Res.*, *108*(D15), 8630, doi:10.1029/2002JD002679, in press, 2003.
- Raes, F., T. Bates, F. McGovern, and M. Van Liederkerke, The 2nd Aerosol Characterization Experiment (ACE-2), General overview and main results, *Tellus, Ser. B*, *52*, 111–125, 2000.
- Schröder, M., R. Bennartz, L. Schüller, R. Preusker, P. Albert, and J. Fischer, Generating cloud masks in spatial high-resolution observations of clouds using texture and radiance information, *Int. J. Remote Sens.*, *23*, 4247–4261, 2002.
- Schüller, L., Retrieval of cloud parameters for indirect aerosol effect studies from spaceborne imaging systems, paper presented at the 6th Scientific Conference of the International Global Atmospheric Chemistry Project (IGAC), IGAC, CNR Inst. for Atmos. and Oceanic Sci. (ISAO), and Eur. Comm., DG XII-JRC, Bologna, Italy, 1999.
- Schüller, L., W. Arnbruster, and J. Fischer, Retrieval of cloud optical and microphysical properties from multi-spectral radiances, *Atmos. Res.*, *55*, 35–46, 2000.
- Schüller, L., J.-L. Brenguier, and H. Pawlowska, Retrieval of microphysical, geometrical and radiative properties of marine stratocumulus from remote sensing, *J. Geophys. Res.*, *108*(D15), 8631, doi:10.1029/2002JD002680, in press, 2003.
- Schwartz, S. E., Harsvardhan, and C. M. Benkovitz, Influence of anthropogenic aerosol on cloud optical depth and albedo shown by satellite measurements and chemical transport modelling, *Proc. Natl. Acad. Sci. U. S. A.*, *99*, 1784–1789, 2002.
- Snider, J., S. Guibert, J.-L. Brenguier, and J.-P. Putaud, Aerosol activation in marine stratocumulus clouds: 2. Köhler and parcel theory closure studies, *J. Geophys. Res.*, *108*(D15), 8629, doi:10.1029/2002JD002692, in press, 2003.
- Twomey, S., The influence of pollution on the shortwave albedo of clouds, *J. Atmos. Sci.*, *34*, 1149–1152, 1977.
- Twomey, S., and T. Cocks, Remote sensing of cloud parameters from spectral reflectance measurements in the near-infrared, *Beitr. Phys. Atmos.*, *62*, 172–179, 1989.
- Verver, G., F. Raes, D. Vogelegang, and D. Johnson, The 2nd Aerosol Characterization Experiment (ACE-2), Meteorological and chemical context, *Tellus, Ser. B*, *52*, 126–140, 2000.
- Warner, J., and S. Twomey, The production of cloud nuclei by cane fires and the effect on cloud drop concentrations, *J. Atmos. Sci.*, *24*, 704–706, 1967.

J.-L. Brenguier, Centre National de Recherche Météorologique (CNRM), GMEI/D, Météo-France, F-31057 Toulouse Cedex 01, France. (jlb@meteo.fr)

H. Pawlowska, Institute of Geophysics, Warsaw University, ul. Pasteura 7, 02-093 Warsaw, Poland. (hanna.pawlowska@igf.fuw.edu.pl)

L. Schüller, Institut für Weltraumwissenschaften, Freie Universität Berlin, Carl-Heinrich-Becker-Weg 6–10, D-12165 Berlin, Germany. (lothar.schueller@wew.fu-berlin.de)